J. COMBIN. MATH. COMBIN. COMPUT. 127b (2025) 8959--8977

Journal of Combinatorial Mathematics
and Combinatorial Computing
www.combinatorialpress.com/jcmcc

Analysis of thermodynamic behavior of high-speed mechanical devices by finite difference method

Linli Sun[1, ✉], Qingsu Liu[1], Haotian Pu[1], Jizheng Pan[1], Zihan Wang[1], Qiukai Xie[1]

[1] *Shaanxi University of Science & Technology, Xi'an, Shaanxi, 710068, China*

ABSTRACT

This paper firstly starts from the thermodynamic theory, based on the classical heat transfer theory, and adopts the finite difference dichotomy method for mathematical modeling, and uses the second-order center difference format to discretize the space, and solves the non-Fourier heat conduction equation. After completing the algorithmic solution of thermodynamic theory and finite difference method, the two are combined to deeply analyze and discuss the thermodynamic behavior of high-speed mechanical devices represented by high-speed rotating bearings. When the bearings operate at high speed, with the increase of stiffness, the pressure change in the middle and rear part of the bearings gradually flattens out, the temperature gradually rises, and the relative bearing capacity of the bearings decreases. The increase in the number of bearings also brings about an increase in the pressure at the centerline of the bearings, and the temperature of the air film corresponds to the increase in the average pressure, and there is a risk of over-temperature. In the thermodynamic characterization, the work done by the air film under compression and the heat generation due to viscous shear will lead to an increase in the temperature of the air film, which will lead to the temperature rise of the bearings, and will have a very great impact on the bearing performance.

Keywords: thermodynamics, heat transfer, non-Fourier heat conduction equation, finite difference method, high-speed mechanical devices

1. Introduction

The finite difference method is a recent achievement in the field of mathematics, which can get very good results in some specific cases. The so-called finite difference equation is to use the integral and difference formula to make the difference equation into a combination of multiple equivalent partial differential equations [1-4], and then apply the optimization method to solve this system of equations, so as to derive the approximate value of the unknown, which is of great significance in the analysis of thermodynamic behaviors of high-speed mechanical devices [5-6].

✉ Corresponding author.
E-mail address: 18629197659@163.com (L. Sun).
Received 15 January 2024; Revised 10 March 2024; Accepted 30 November 2024; Published Online 16 April 2025.
DOI: 10.61091/jcmcc127b-492

Thermodynamics is the study of the nature of matter under the action of heat and the law of change of science. The object of its study is the nature of macroscopic substances and the interaction between them, which mainly involves the concepts of energy, heat, work, thermal efficiency, etc., and is widely used in various fields [7-10]. And in mechanical systems, the application of thermodynamic properties covers several fields. The first one is heat engines and heat energy conversion devices. Through thermodynamic analysis, the thermal efficiency and power output of heat engines can be evaluated to guide the design improvement of thermal energy conversion devices [11-14]. Next is the cooling system and thermal management. Through thermodynamic analysis, suitable cooling media and cooling methods can be determined to improve the heat dissipation efficiency of mechanical systems [15-16]. In addition, the application of thermodynamics in energy engineering and materials science is also very important to optimize energy use and material properties. The application of thermodynamics in mechanical systems can help us to gain a deeper understanding of energy transformations and analyze the power output and heat loss of a system [17-20]. The application of thermodynamics can not only improve the energy utilization efficiency of mechanical systems, but also provide guidance for the development of new energy technologies. With the progress of science and technology, the application of thermodynamics in mechanical systems will usher in more challenges and opportunities [21-24].

This paper puts the research attention to the high-speed mechanical devices, and takes its thermodynamic behavior as the entry point of this research. Firstly, the theoretical basis of this research - the principle of thermodynamics is discussed. Heat transfer is attributed to the module of the second law of thermodynamics, and it is proposed to determine the expression formula of heat conduction through Fourier's law in accordance with the three basic processes of heat transfer, namely, heat conduction, convective heat transfer and radiative heat transfer. In order to obtain the heat balance to calculate the friction force, heat generation per unit time and other indicators, the effective temperature is solved using the running curve method, and isothermal calculations are carried out under the assumption that the temperature in the oil film is homogeneous. The finite difference analysis method is used as a means of analyzing the thermodynamic behavior of high-speed mechanical devices in this study, and the finite difference method is used to solve the non-Fourier heat transfer equation. Based on the precondition that the non-Fourier heat conduction is unsteady state heat conduction, the solution area is discretized, the partial differential equations satisfied by the temperature field are calculated, the initial and boundary conditions are determined, and the solution of the non-Fourier heat conduction equations is finally completed. Taking the principle of thermodynamics as the theoretical basis, using the finite difference method and its mathematical model as the means, selecting the high-speed rotating bearing in the high-speed mechanical device as the representative, and determining the research type as the gas bearing, we carry out the thermodynamic behavior analysis of the high-speed mechanical device.

2. Thermodynamics of high-speed mechanical devices

Heat transfer is the process of transferring heat due to temperature difference, called heat transfer, which follows the second law of thermodynamics [25-26]. Wherever there is a temperature difference, there must be heat transfer, and thus it is an extremely common energy conversion process in engineering and technology.

If the heat transfer is not taken into account, that is, assuming that the temperature in the oil film is uniform, i.e., isothermal calculations, this is one of the simplest ideal processes.

2.1. Basic process of heat transfer

Heat transfer is a complex process that is usually analyzed and studied according to three basic processes: heat conduction, convective heat transfer and radiative heat transfer. Any kind of complex heat transfer phenomenon, perhaps can be reduced to two or even a certain kind of heat transfer process and the corresponding heat transfer calculations.

The process by which heat is transferred from a high-temperature part of an object to a low-temperature part, or from a high-temperature object to a low-temperature object with which it is in direct contact, is known as heat conduction or heat transfer. It is a process of heat transfer caused by microscopic movements of molecules, atoms and free electrons, which takes place in gases, liquids and solids. In a purely thermally conductive process, there is no macroscopic motion between the parts of an object.

The basic law of thermal conductivity is expressed by Fourier's law, i.e. [27]:

$$q_n = -\lambda \frac{\partial T}{\partial n} \tag{1}$$

where q_n - density of heat flow in the direction normal to the isothermal surface, W/m^2.

λ - thermal conductivity (rate), $W/m/K$.

$\frac{\partial T}{\partial n}$ - temperature gradient in the direction normal to the isothermal surface, K/m.

The negative sign in equation (1) indicates that the direction of heat transfer is opposite to the direction of the temperature gradient. Thermal conductivity λ is a physical parameter characterizing the thermal conductivity of the material, which is mainly related to the type of material and temperature, the thermal conductivity of specific materials can be queried for relevant information to obtain.

2.2. *Effective temperature for isothermal assumptions*

The earliest consideration of temperature effects in the design of bearings in mechanical devices was based on the assumption of isothermal, using the weighted “effective temperature” as the temperature of the entire temperature field, which can be calculated by heat balance. The effective temperature in the oil film should be greater than its oil temperature, otherwise, such as low temperature, viscosity, calculated pressure, load carrying capacity and friction power is large, while the flow rate is small, which is unsafe. Therefore, it is necessary to calculate the performance of the bearing according to the thermal balance of the whole oil film in order to be closer to the actual value.

In order to find the heat balance, on the one hand, the friction generated in the bearing F_f should be calculated, and the heat generation per unit of time ϕ_t can be obtained, on the other hand, the heat carried away by the lubricant from the bearing ϕ_a, and the heat emitted through the rotor and bearing seat ϕ_λ, both should be equal, i.e.:

$$\phi_t = \phi_a + \phi_\lambda \tag{2}$$

And:

$$\phi_t = F_f U \tag{3}$$

Cole and Dawson's experiments can be seen, the bearing by the oil to take away the heat is much larger than the conduction heat dissipation, the higher the shaft speed is more obvious. In order to simplify and assume that the “adiabatic flow”, that is, all the heat is absorbed by the oil and taken away by the end of the leakage, heat and end of the leakage heat balance, get:

$$F_f U = Q_b \rho c_v \Delta T \tag{4}$$

To wit:

$$\Delta T = F_f U / \left(Q_b \rho c_v\right) \tag{5}$$

Set the inlet oil temperature T_{in}, then the outlet oil temperature:

$$T_{out} = T_{in} + \Delta T \tag{6}$$

In bearing design, if non-adiabatic assumptions are made, the effective temperature can be solved using the running curve method to take into account the effect of temperature rise.

If the type and size of the bearing are certain, under a given operating condition, the end drain flow Q_b and power P, i.e. the heat generated per unit of time, are calculated by assuming that the viscosity η is a constant. It is also assumed that the heat carried away by convection of the oil $k_l P$, $0 < k_l < 1$. The rest of the heat $(1-k_l)P$ is dissipated by heat conduction. Balance by heat:

$$k_1 P = Q_b \rho c_v \Delta T \tag{7}$$

At this point, the effective temperature of the bearing:

$$T = T_0 + k\Delta T \tag{8}$$

where: k - another constant different from k_l.

T_0 - the initial temperature of the oil, i.e. the inlet temperature.

Combined with the calculations carried out on the thrust tile block bearings and experimental evidence, the average temperature of the oil out of the oil T_{out} as the effective temperature of the oil film T, and according to the isothermal assumptions for calculating the load carrying capacity is available, namely

$$T = T_{out} \tag{9}$$

For low and medium speed bearings, it is appropriate to take slightly lower than the oil discharge temperature as the effective temperature, considering conduction heat dissipation, and Cameron recommends taking it:

$$T = T_0 + 0.8\Delta T \tag{10}$$

3. Finite difference method and mathematical modeling

3.1. Principle of Finite Difference Method

Finite difference method (FDM) is an early developed and more mature numerical method, which is a numerical solution method that transforms differential problems into algebraic problems [28]. It first grids the solution domain, and then uses Taylor series expansions, etc. to carry out the derivatives in the equations required to be solved by the difference quotients of the function values at the grid nodes, thus creating a series of algebraic equations with the values at the grid nodes as the unknowns. Divided according to the accuracy of the format, it includes first-order format, second-order format, and higher-order format. According to the spatial form of the difference, it includes the center difference format, the backward difference format, and the upwind difference format, and so on. According to the division of the influence of time factor, it includes explicit format, implicit format, and explicit-implicit alternating format, and so on. At present, the frequently used difference format is generally a combination of the above formats, and different combinations can constitute different difference formats. The finite difference method is mainly applicable to structured meshes, and we can decide the step size of the mesh according to the actual geometry and the Crown stability conditions. The current method to construct the difference is mainly the Taylor series expansion method. Its basic difference expressions include the following forms: first-order backward difference method, first-order center difference method, second-order backward difference method, and second-order center difference method, etc., of which the first two formats are for the first-order computational accuracy, and the last two formats are for the second-order computational accuracy. By combining these different difference formats in time and space, different difference calculation formats can be combined.

Replacing the differential quotient with the differential quotient is the mathematical basis for finite difference, i.e., replacing the derivative with the finite difference. If $f(x)$ is a continuous function, its derivative can be expressed as:

$$\frac{df}{dx} = \lim_{\Delta x \to 0} \frac{f(x+\Delta x) - f(x)}{\Delta x} = \lim_{\Delta x \to 0} \frac{\Delta f}{\Delta x} \tag{11}$$

A Taylor series expansion can be used to obtain a finite difference approximate expression for the derivative of a function. Let $f(x)$ be expanded into a Taylor series, then we have [29]:

$$f(x+\Delta x) = f(x) + \Delta x \frac{df}{dx} + \frac{(\Delta x)^2}{2!} + \cdots \tag{12}$$

$$f(x-\Delta x) = f(x) - \Delta x \frac{df}{dx} + \frac{(\Delta x)^2}{2!} + \cdots \tag{13}$$

Rewriting each of the above two equations gives:

$$\frac{df}{dx} = \frac{f(x+\Delta x) - f(x)}{\Delta x} - \frac{\Delta x}{2}\frac{d^2 f}{dx^2} - \frac{(\Delta x)^2}{6}\frac{d^3 f}{dx^3} - \cdots \tag{14}$$

$$\frac{df}{dx} = \frac{f(x) - f(x-\Delta x)}{\Delta x} + \frac{\Delta x}{2}\frac{d^2 f}{dx^2} - \frac{(\Delta x)^2}{6}\frac{d^3 f}{dx^3} - \cdots \tag{15}$$

According to (12)~(15) the approximate expressions for the finite difference quotient of the first-order forward difference, the first-order backward difference, the first-order center difference, and the second-order center difference of the function $f(x)$ at the point x can be written, respectively:

$$\frac{df}{dx} = \frac{f(x+\Delta x) - f(x)}{\Delta x} + O(\Delta x) \tag{16}$$

$$\frac{df}{dx} = \frac{f(x) - f(x-\Delta x)}{\Delta x} + O(\Delta x) \tag{17}$$

$$\frac{df}{dx} = \frac{f(x+\Delta x) - f(x-\Delta x)}{2\Delta x} + O(\Delta x) \tag{18}$$

$$\frac{df}{dx} = \frac{f(x+\Delta x) - 2f(x) + f(x-\Delta x)}{2\Delta x} + O(\Delta x)^2 \tag{19}$$

where $O(\Delta x)$ is the error of replacing the minimizer by the difference quotient, i.e., the error caused by rounding off the higher order terms of the Taylor series, called the truncation error. Here O denotes the order of magnitude, and $O(\Delta x)$ indicates that this truncation error is a small quantity of the same order of magnitude as Δx. The truncation error of the center difference format is of order $(\Delta x)^2$.

In case of cylindrical coordinate system, the finite difference quotient approximation expressions for first order backward difference and second order difference formats are:

$$\frac{df}{dr} = \frac{f(r) - f(r-\Delta r)}{\Delta r} + O(\Delta r) \tag{20}$$

$$\frac{df}{dr} = \frac{f(r+\Delta r) - 2f(r) + f(\Delta r)}{2\Delta r} + O(\Delta r)^2 \tag{21}$$

3.2. Mathematical model analysis

In order to solve numerically, we should first discretize the solution region, because non-Fourier heat conduction is non-stationary thermal conductivity, and the change of temperature field is not only space-dependent but also time-dependent, so the discretization of the solution region involves not only the discretization of the spatial coordinates, but also the need to discretize the time. The finite difference method requires the use of orthogonal mesh in the right-angled coordinate system is a rectangular grid, with two families of parallel straight lines $x = x_m = mh(m = 1, 2, \cdots, M)$ and $t = t_n = n\tau(n = 1, 2, \cdots, N)$ to partition the rectangular region $G = \{0 \le x \le l, 0 \le t \le T\}$ into a rectangular grid, the intersection of the mesh lines is called a node, nodes within the region is called an internal node, nodes falling on the boundary is a boundary node, and the distance between the lines of the mesh is called the step size.

Next denote by T_m^n the function defined at node (x_m, t_n). So for a one-dimensional temperature response $T = T(x,t)$, the appropriate spatial step Δx and time step Δt are chosen, and the numerical analysis is the transformation of a problem to find a continuous function $T = T(x,t)$ into a discretized problem to find the temperature value T_m^n at a specific node at a specific time interval $(x = m\Delta x, t = n\Delta t)$.

The direction x is the thickness direction of the plywood, assuming that the thickness of the first layer of material is L_1 and the thickness of the second layer of material is L_2. The initial temperature of the plywood is 0 °C, and the left surface $(x = 0)$ of the plywood is subjected to a transient temperature $T_0\left(T_0 > 0\right)$, while the temperature of the right surface $\left(x = L_1 + L_2\right)$ remains 0 °C. The temperature of the plywood at point 1 is 0 °C, and the temperature of the right surface is 0 °C. We denote by $T(x,t)$ the transient temperature at point (x,t), which is a continuous function of spatial coordinate x and time coordinate t. Assuming that the heat propagates only in the thickness direction, the temperature field $T(x,t)$ satisfies the following partial differential equation according to the non-Fourier heat conduction theory:

$$\tau_1 \frac{\partial^2 T}{\partial t^2} + \frac{\partial T}{\partial t} = k_1 \frac{\partial^2 T}{\partial x^2} \tag{22}$$

$$\tau_2 \frac{\partial^2 T}{\partial t^2} + \frac{\partial T}{\partial t} = k_2 \frac{\partial^2 T}{\partial x^2} \tag{23}$$

where τ_1 and τ_2 are relaxation times, k_1 and k_2 are thermal diffusivities also known as thermal conductivity coefficients $\left(m^2 / s\right)$, and the subscripts 1 and 2 refer to the first and second layer materials, respectively.

The initial and boundary conditions are respectively:

$$T(x,t)\big|_{x=0} = T_0, t > 0 \tag{24}$$

$$T(x,t)\big|_{x-L_1+L_2} = 0, t > 0 \tag{25}$$

$$T(x,t)\big|_{t=0} = 0, 0 \le x \le L_1 + L_2 \tag{26}$$

$$\partial T(x,t) / \partial t\big|_{t=0} = 0, 0 \le x \le L_1 + L_2 \tag{27}$$

Since the object is homogeneous along the thickness direction, the temperature of each part of the cross section perpendicular to the thickness direction is equal, i.e., the cross section perpendicular to the thickness direction can be regarded as a point, and by dividing the first layer of the material into M_1 part along the thickness direction, and the second layer into $M - M_1$, the whole material is divided into M parts, and the intersection of the two layers of material is the $M_1 + 1$th point.

The second order partial derivative with respect to coordinate x is approximated by the center difference at moment t:

$$\frac{\partial^2 T_m^n}{\partial x^2} = \frac{T_{m-1}^n - 2T_m^n + T_{m+1}^n}{(\Delta x)^2} \tag{28}$$

The difference quotient is approximated:

$$\tau_1 \frac{\partial^2 T_m^n}{\partial t^2} + \frac{\partial T_m^n}{\partial t} = k_1 \frac{T_{m+1}^n - 2T_m^n + T_{m-1}^n}{(\Delta x)^2}, m = 2, 3, \cdots, M_1 \tag{29}$$

$$\begin{gathered} \tau_2 \frac{\partial^2 T_m^n}{\partial t^2} + \frac{\partial T_m^n}{\partial t} = k_2 \frac{T_{m+1}^n - 2T_m^n + T_{m-1}^n}{(\Delta x)^2} \\ m = M_1 + 2, M_1 + 3, \cdots\cdots, M \end{gathered} \tag{30}$$

For the point at the junction of the two materials, we take $\tau = \frac{\tau_1 + \tau_2}{2}$, $k = \frac{k_1 + k_2}{2}$ then

$$\frac{\tau_1 + \tau_2}{2} \frac{\partial^2 T_m^n}{\partial t^2} + \frac{\partial T_m^n}{\partial t} = \frac{k_1 + k_2}{2} \frac{T_{m+1}^n - 2T_m^n + T_{m-1}^n}{(\Delta x)^2}, m = M_1 + 1 \tag{31}$$

Eqs. (28), (29), and (30) can be written as respectively:

$$\begin{gathered} \begin{pmatrix} 0 & \tau_1 & 0 \end{pmatrix} \begin{pmatrix} \ddot{T}_{m-1}^n \\ \ddot{T}_m^n \\ \ddot{T}_{m+1}^n \end{pmatrix} + \begin{pmatrix} 0 & 1 & 0 \end{pmatrix} \begin{pmatrix} \dot{T}_{m-1}^n \\ \dot{T}_m^n \\ \dot{T}_{m+1}^n \end{pmatrix} \\ + \begin{pmatrix} -\frac{k_1}{(\Delta x)^2} & \frac{2k_1}{(\Delta x)^2} & -\frac{k_1}{(\Delta x)^2} \end{pmatrix} \begin{pmatrix} T_{m-1}^n \\ T_m^n \\ T_{m+1}^n \end{pmatrix} = 0 \end{gathered} \tag{32}$$

Among them:

$$m = 1, 2, \cdots, M_1 \tag{33}$$

$$\begin{pmatrix} 0 & \tau_2 & 0 \end{pmatrix} \begin{pmatrix} \ddot{T}_{m-1}^n \\ \ddot{T}_m^n \\ \ddot{T}_{m+1}^n \end{pmatrix} + \begin{pmatrix} 0 & 1 & 0 \end{pmatrix} \begin{pmatrix} \dot{T}_{m-1}^n \\ \dot{T}_m^n \\ \dot{T}_{m+1}^n \end{pmatrix} + \begin{pmatrix} -\frac{k_2}{(\Delta x)^2} & \frac{2k_2}{(\Delta x)^2} & -\frac{k_2}{(\Delta x)^2} \end{pmatrix} \begin{pmatrix} T_{m-1}^n \\ T_m^n \\ T_{m+1}^n \end{pmatrix} = 0 \tag{34}$$

Among them:

$$m = M_1 + 2, M_1 + 3, \cdots, M \tag{35}$$

$$\begin{gathered} \begin{pmatrix} 0 & \frac{\tau_1 + \tau_2}{2} & 0 \end{pmatrix} \begin{pmatrix} \ddot{T}_{m-1}^n \\ \ddot{T}_m^n \\ \ddot{T}_{m+1}^n \end{pmatrix} + \begin{pmatrix} 0 & 1 & 0 \end{pmatrix} \begin{pmatrix} \dot{T}_{m-1}^n \\ \dot{T}_m^n \\ \dot{T}_{m+1}^n \end{pmatrix} \\ + \begin{pmatrix} -\frac{k_1 + k_2}{2(\Delta x)^2} & \frac{k_1 + k_2}{(\Delta x)^2} & -\frac{k_1 + k_2}{2(\Delta x)^2} \end{pmatrix} \begin{pmatrix} T_{m-1}^n \\ T_m^n \\ T_{m+1}^n \end{pmatrix} = 0 \end{gathered} \tag{36}$$

Among them:

$$m = M_1 + 1 \tag{37}$$

Since $T_1^n = T_0$ is constant when $m = 1$; and $T_{M+1}^n = 0$ is the initial boundary condition when $m = M + 1$, there is:

$$\begin{pmatrix}\tau_1 & 0\end{pmatrix}\begin{pmatrix}\ddot{T}_2^n \\ \ddot{T}_3^n\end{pmatrix}+\begin{pmatrix}1 & 0\end{pmatrix}\begin{pmatrix}\dot{T}_2^n \\ \dot{T}_3^n\end{pmatrix}+\begin{pmatrix}\frac{2k_1}{(\Delta x)^2} & -\frac{k_1}{(\Delta x)^2}\end{pmatrix}\begin{pmatrix}T_2^n \\ T_3^n\end{pmatrix}=\frac{k_1}{(\Delta x)^2}T_0 \tag{38}$$

$$\begin{pmatrix}0 & \tau_2\end{pmatrix}\begin{pmatrix}\ddot{T}_{M-1}^n \\ \ddot{T}_M^n\end{pmatrix}+\begin{pmatrix}0 & 1\end{pmatrix}\begin{pmatrix}\dot{T}_{M-1}^n \\ \dot{T}_M^n\end{pmatrix}+\begin{pmatrix}-\frac{k_2}{(\Delta x)^2} & \frac{2k_2}{(\Delta x)^2}\end{pmatrix}\begin{pmatrix}T_{M-1}^n \\ T_M^n\end{pmatrix}=\frac{k_2}{(\Delta x)^2}T_{M+1}^n=0 \tag{39}$$

Jointly (23)~(27) yields:

$$\begin{aligned}&\begin{pmatrix}\tau_1 & 0 & & & \\ 0 & \tau_1 & 0 & & \\ & \ddots & \ddots & \ddots & \\ & & 0 & \tau_1 & 0\end{pmatrix}\begin{pmatrix}\ddot{T}_2^n \\ \vdots \\ \ddot{T}_{M_1+1}^n\end{pmatrix}+\begin{pmatrix}1 & 0 & & & \\ 0 & 1 & 0 & & \\ & \ddots & \ddots & \ddots & \\ & & 0 & 1 & 0\end{pmatrix}\begin{pmatrix}\dot{T}_2^n \\ \vdots \\ \dot{T}_{M_1+1}^n\end{pmatrix}\\ &+\begin{pmatrix}\frac{2k_1}{(\Delta x)^2} & -\frac{k_1}{(\Delta x)^2} & & & \\ -\frac{k_1}{(\Delta x)^2} & \frac{2k_1}{(\Delta x)^2} & -\frac{k_1}{(\Delta x)^2} & & \\ & \ddots & \ddots & \ddots & \\ & & -\frac{k_1}{(\Delta x)^2} & \frac{2k_1}{(\Delta x)^2} & -\frac{k_1}{(\Delta x)^2}\end{pmatrix}\begin{pmatrix}T_2^n \\ \vdots \\ T_{M_1+1}^n\end{pmatrix}=\begin{pmatrix}\frac{k_1}{(\Delta x)^2}T_0 \\ 0 \\ \vdots \\ 0\end{pmatrix}\end{aligned} \tag{40}$$

$$\begin{aligned}&\begin{pmatrix}0 & \frac{\tau_1+\tau_2}{2} & 0\end{pmatrix}\begin{pmatrix}\ddot{T}_{m-1}^n \\ \ddot{T}_m^n \\ \ddot{T}_{m+1}^n\end{pmatrix}+\begin{pmatrix}0 & 1 & 0\end{pmatrix}\begin{pmatrix}\dot{T}_{m-1}^n \\ \dot{T}_m^n \\ \dot{T}_{m+1}^n\end{pmatrix}\\ &+\begin{pmatrix}-\frac{k_1+k_2}{2(\Delta x)^2} & \frac{k_1+k_2}{(\Delta x)^2} & -\frac{k_1+k_2}{2(\Delta x)^2}\end{pmatrix}\begin{pmatrix}T_{m-1}^n \\ T_m^n \\ T_{m+1}^n\end{pmatrix}=0\end{aligned} \tag{41}$$

$$\begin{aligned}&\begin{pmatrix}0 & \tau_2 & 0 & & \\ & 0 & \tau_2 & \ddots & \\ & & \ddots & \ddots & 0 \\ & & & 0 & \tau_2\end{pmatrix}\begin{pmatrix}\ddot{T}_{M_1+1}^n \\ \vdots \\ - \\ \ddot{T}_M^n\end{pmatrix}+\begin{pmatrix}0 & 1 & 0 & & \\ & 0 & 1 & \ddots & \\ & & \ddots & \ddots & 0 \\ & & & 0 & 1\end{pmatrix}\begin{pmatrix}\dot{T}_{M_1+1}^n \\ \vdots \\ \dot{T}_M^n\end{pmatrix}\\ &+\begin{pmatrix}-\frac{k_2}{(\Delta x)^2} & \frac{2k_2}{(\Delta x)^2} & -\frac{k_2}{(\Delta x)^2} & & \\ & \frac{k_2}{(\Delta x)^2} & \frac{2k_2}{(\Delta x)^2} & \ddots & \\ & & \ddots & \ddots & -\frac{k_2}{(\Delta x)^2} \\ & & & -\frac{k_2}{(\Delta x)^2} & \frac{2k_2}{(\Delta x)^2}\end{pmatrix}\begin{pmatrix}T_{M_1+1}^n \\ \vdots \\ T_M^n\end{pmatrix}=\begin{pmatrix}0 \\ \vdots \\ 0\end{pmatrix}\end{aligned} \tag{42}$$

Order:

$$K=\begin{bmatrix} \frac{2k_1}{(\Delta x)^2} & -\frac{k_1}{(\Delta x)^2} & & & & & & & \\ -\frac{k_1}{(\Delta x)^2} & \ddots & \ddots & & & & & & \\ & \ddots & \ddots & \ddots & & & & & \\ & & -\frac{k_1}{(\Delta x)^2} & \frac{2k_1}{(\Delta x)^2} & -\frac{k_1}{(\Delta x)^2} & & & & \\ & & & -\frac{k_1+k_2}{2(\Delta x)^2} & \frac{k_1+k_2}{(\Delta x)^2} & -\frac{k_1+k_2}{2(\Delta x)^2} & & & \\ & & & & -\frac{k_2}{(\Delta x)^2} & \frac{2k_2}{(\Delta x)^2} & -\frac{k_2}{(\Delta x)^2} & & \\ & & & & & \ddots & \ddots & & \\ & & & & & & \ddots & & \\ & & & & & & -\frac{k_2}{(\Delta x)^2} & \frac{2k_2}{(\Delta x)^2} \end{bmatrix} \tag{43}$$

where K is a tridiagonal matrix of order $(M-1)\times(M-1)$:

$$P=\begin{pmatrix} \frac{k_1}{(\Delta x)^2}T_0 \\ 0 \\ \vdots \\ 0 \end{pmatrix}_{(M-1)}, C=\begin{pmatrix} 1 & & \\ & \ddots & \\ & & 1 \end{pmatrix}_{(M-1)\times(M-1)}$$

$$D=\begin{pmatrix} \tau_1 & & & & & & \\ & \ddots & & & & & \\ & & \tau_1 & & & & \\ & & & \frac{\tau_1+\tau_2}{2} & & & \\ & & & & \tau_2 & & \\ & & & & & \ddots & \\ & & & & & & \tau_2 \end{pmatrix}_{(M-1)\times(M-1)} \tag{44}$$

Then we can write (42), (43) jointly with (44) as:

$$D\begin{pmatrix} \ddot{T}_2^n \\ \vdots \\ \ddot{T}_M^n \end{pmatrix}+C\begin{pmatrix} \dot{T}_2^n \\ \vdots \\ \dot{T}_M^n \end{pmatrix}+K\begin{pmatrix} T_2^n \\ \vdots \\ T_M^n \end{pmatrix}=P \tag{45}$$

4. Thermodynamic analysis of high-speed mechanical devices based on the finite difference method

High-speed mechanical devices are usually required to operate at high rotational speeds to achieve higher productivity and processing accuracy. At present, there are more and more ultra-high-speed operation scenarios represented by new energy automobile electric drive system, aviation engine, etc., and the performance requirements for high-speed mechanical devices and components are also increasing. High-speed rotating bearings, as one of the commonly used core components in high-speed mechanical devices, have been put forward with higher requirements for temperature rise control.

Based on thermodynamic principles, this study will analyze and discuss the thermodynamic behavior of high-speed mechanical devices represented by high-speed rotating bearings through the finite difference method.

The selected high-speed rotating bearing type is gas bearing. Gas bearings have the advantages of high speed, low power consumption, no pollution, wide range of operating temperature and so on, which get rid of the limitations of liquid lubricated bearings in terms of rotational speed and temperature, and the application prospect is broad, which has high research significance.

4.1. Bearing performance impact analysis

4.1.1. Effect of stiffness and temperature on bearing performance. When the bearing carries out high-speed operation, the pressure at the centerline of the bearing and the change of the rigid part are shown specifically in Fig. 1. Figures (a) and (b) show the pressure change at the centerline of the bearing and the average pressure change, respectively. From the figures, it can be seen that at low stiffness, the pressure at the middle and rear part of the bearing is higher, resulting in larger local deformation of the foil. With the increase of stiffness, the pressure change in the middle and rear part of the bearing gradually flattens out. As the stiffness continues to increase, the bearing tends to be a rigid bearing, making the maximum pressure at the junction of inclined and flat surfaces.

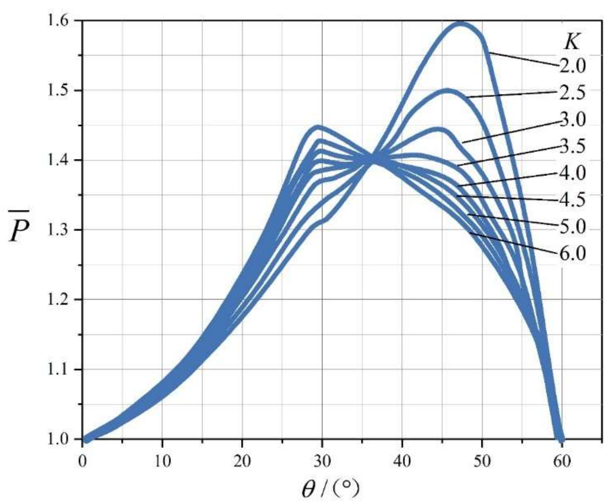

(a)Pressure change in the middle of the bearing

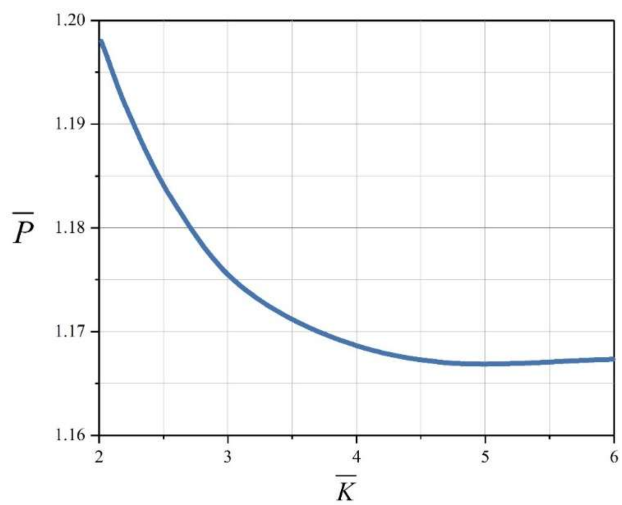

(b)Mean pressure variation

Fig. 1. Change of pressure with stiffness

The variation of temperature and stiffness during the operation of the bearings is specifically shown in Fig. 2, Fig. (a) shows the variation of temperature at the centerline of the bearings, and Fig. (b) shows the variation of the average temperature. From the figure, it can be seen that the stiffness of the bearing shows a positive correlation with the temperature, with the increase of the stiffness, the temperature also increases gradually.

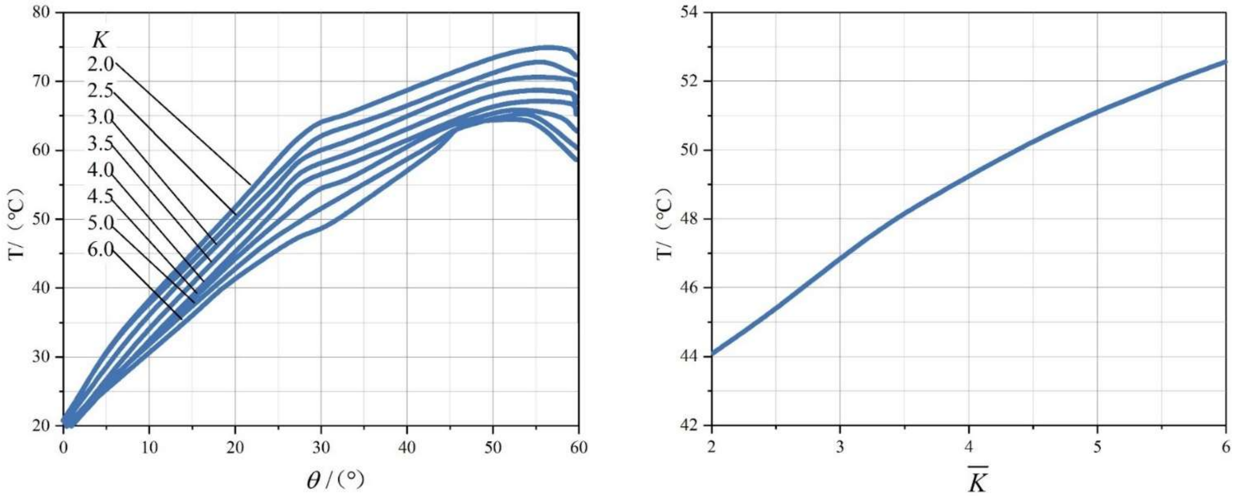

(a)Temperature change in the center of the bearing (b)Mean temperature variation

Fig. 2. Change of temperature with stiffness

The variation of relative bearing capacity with respect to stiffness is specifically shown in Fig. 3. It can be clearly seen that as the stiffness increases, the relative bearing capacity of the bearing decreases continuously, which is consistent with the variation of the average pressure above.

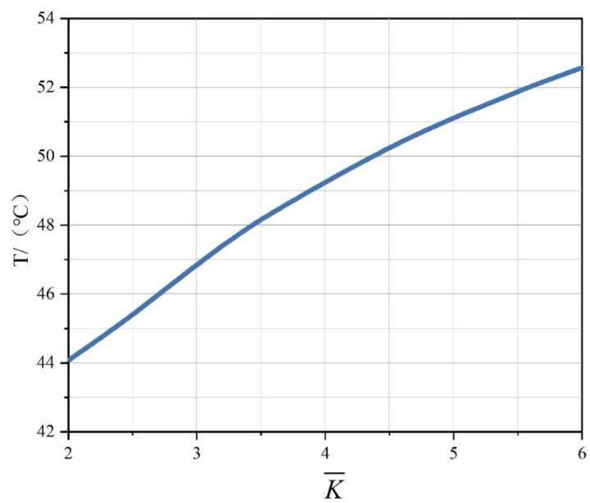

Fig. 3. Relative bearing capacity varies with stiffness

Integration of the above analysis, bearing design needs to consider the stiffness of the elastic foil, in order to ensure that the support structure does not fail for excessive deformation under the appropriate reduction of the stiffness requirements can not only improve the load carrying capacity and adaptability, but also reduce the temperature, reduce the risk of high temperature during high-speed operation of the bearing.

4.1.2. Effect of bearing number and temperature on bearing performance. The variation of pressure at the bearing centerline with respect to the number of bearings is specifically shown in Fig. 4. Figures (a) and (b) show the variation of pressure at the centerline of the bearing and the variation of average pressure, respectively. From the figure, it can be seen that the number of bearings has a greater effect on the pressure, with the increase of the number of bearings, the pressure increases and mainly in the middle and rear of the bearing.

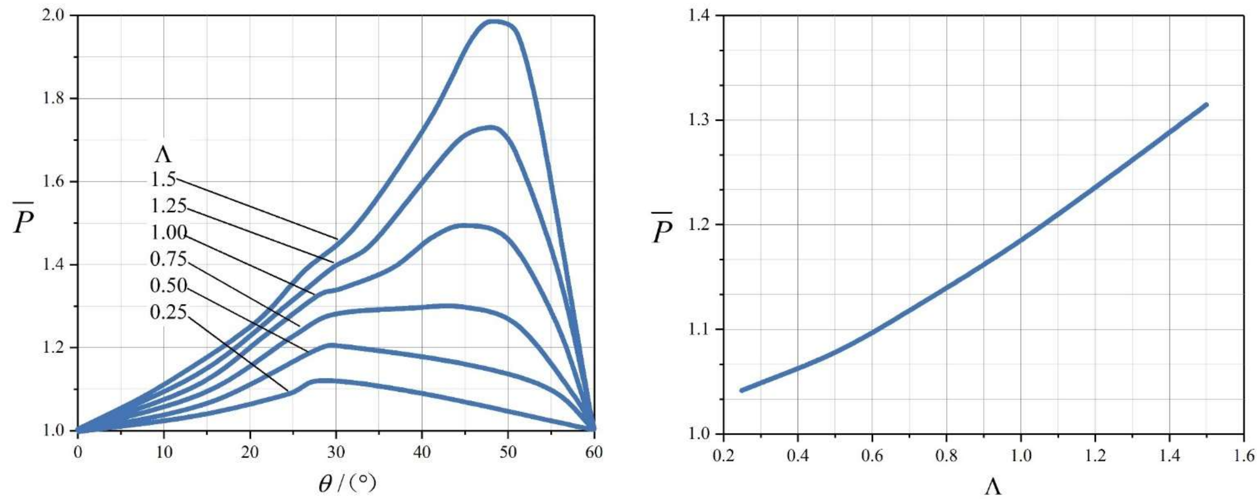

(a)Pressure change in the middle of the bearing (b)Mean pressure variation

Fig. 4. The pressure varies with the number of bearings

The variation of temperature during bearing operation with bearing number is specifically shown in Fig. 5, Figs. (a) and (b) show the variation of temperature at the centerline of the bearing and the variation of average temperature, respectively. At a certain number of bearings, the pressure at the flat foil can reach a uniform distribution, and the gradient of the growth of both the average pressure and the average temperature will increase after exceeding this value.

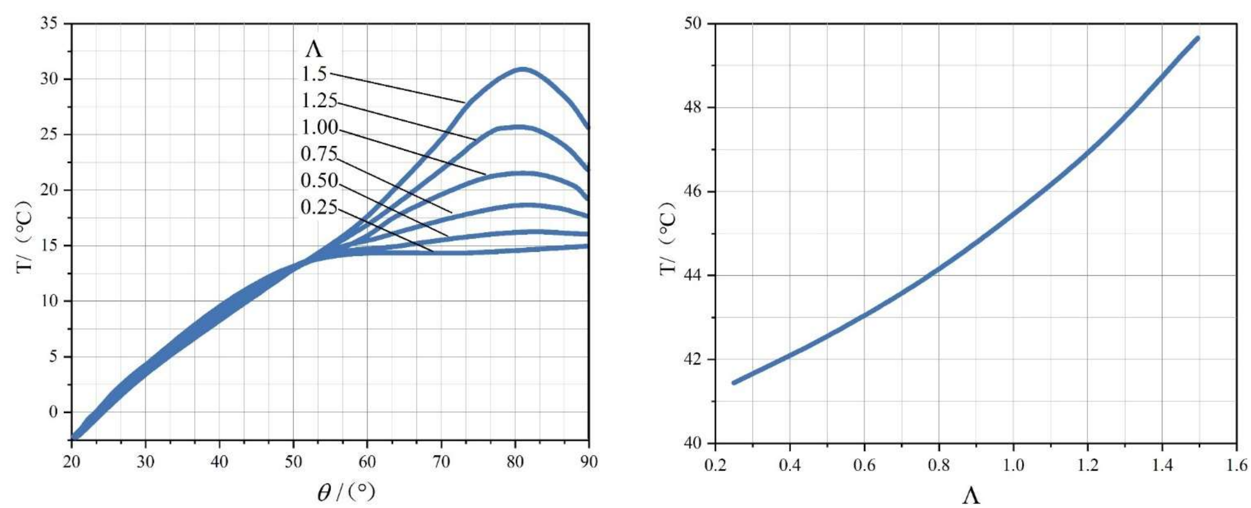

(a)Temperature change in the center of the bearing (b)Mean temperature variation

Fig. 5. Temperature varies with bearing

The relative load carrying capacity varies with the number of bearings as shown in Fig. 6. The trend of change of load carrying capacity with the number of bearings is consistent with the change of average pressure, and the friction torque is positively and linearly correlated with the number of bearings.

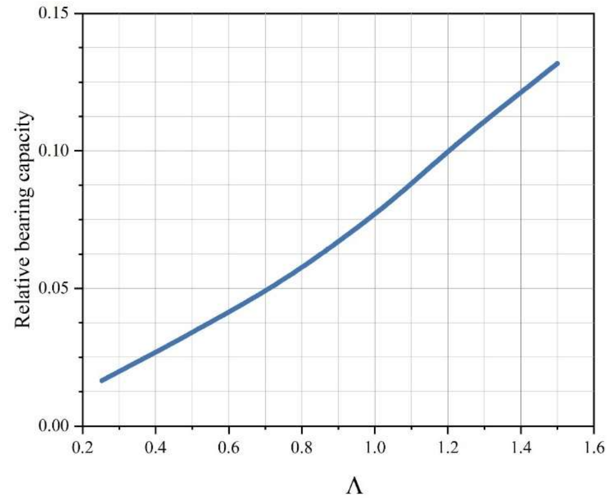

Fig. 6. Relative bearing capacity varies with bearing

Obviously, the number of bearings increases, the temperature of the air film also increases, and the average pressure also increases. Bearing design needs to consider the design of the number of bearings, under the premise of ensuring that the bearing can realize high-speed operation, the number of bearings can be increased appropriately to improve the bearing capacity of the bearings and reduce the high temperature of the existence of hidden dangers and risks.

4.2. Characterization of thermodynamic behavior of bearings

Under normal high-speed operating conditions, there is flow work and action in the gas film between the rotor thrust disk and the bearing surface, which will lead to an increase in the temperature of the gas film. Foil gas thrust bearing lubrication gas film temperature rise will cause lubricating gas density and viscosity changes, the bearing performance has a very big impact. In addition, the temperature rise of the gas film will cause thermal deformation of the bearing element, and the high temperature may even lead to thermal failure of the bearing. Combining the thermodynamic principle of high-speed mechanical device and finite difference method proposed in this paper, the temperature field inside the bearing is predicted and analyzed more accurately with thermodynamic behavioral characteristics, which can provide design guidance reference for the temperature management of the bearing.

4.2.1. Analysis of air film temperature and density distribution. The temperature distribution of the air film in the middle section of the air film in the direction of rotation is shown in Fig. 7. As can be seen from the figure, the temperature of the gas film increases along the film thickness direction from the stationary top foil side to the rotating thrust disk side. This is due to the fact that the gas flow rate near the rotor side is greater than that near the top foil side (the gas flow rate in contact with the top foil is zero when slip is not considered). In addition, the temperature of the gas film near the outer diameter is higher than the temperature of the gas film near the inner diameter.

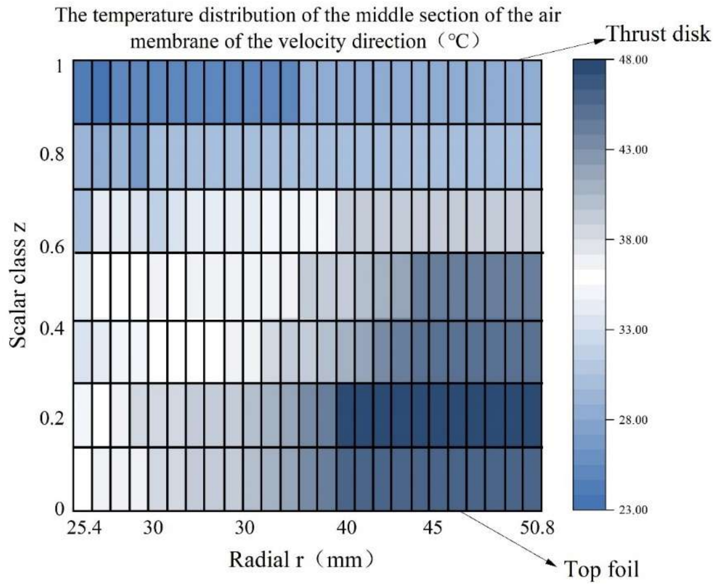

Fig. 7. Gas film temperature profile

The density distribution in the middle cross-section of the gas film in the rotational speed direction is shown in Fig. 8. In the radial direction, the gas density increases and then decreases because the pressure of the gas film increases and then decreases in the radial direction, while the temperature of the gas film increases along the radial direction. In addition, since the pressure gradient in the film thickness direction is neglected in the calculation of the pressure distribution, the temperature near the top foil side is lower than that near the thrust disk side. Therefore, in the film thickness direction, the density of the gas near the top foil is slightly higher than that of the gas near the thrust disk.

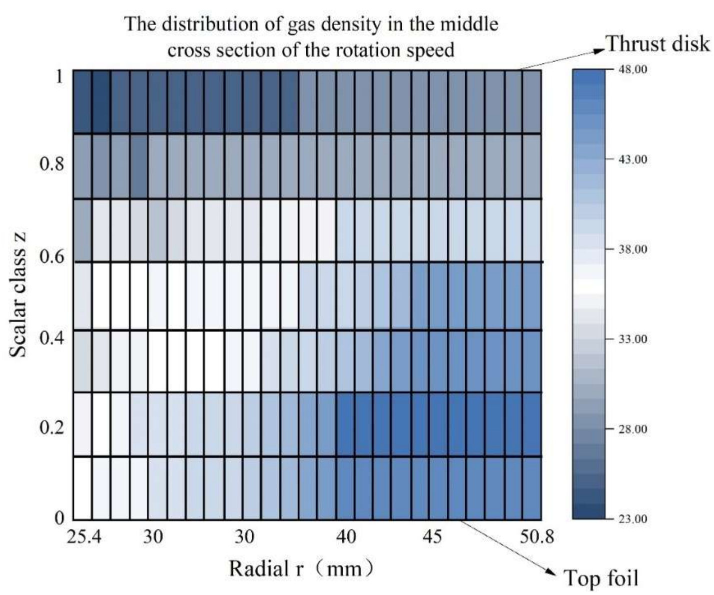

Fig. 8. Density profile

4.2.2. Parametric analysis of thermal characteristics of bearings. The effects of different rotational speeds on the average temperatures of the top foil, the middle gas film and the thrust disk rotor of the foil gas thrust bearings with an axial load of 100 N and no cooling are shown in Fig. 9. The graphs show that the temperatures of the top foil, the intermediate gas film and the thrust disk rotor all increase parabolically with the increase of rotational speed. Under the same rotational speed, load and cooling conditions, the temperature of the thrust disk is higher than that of the intermediate air film, and the temperature of the intermediate air film is higher than that of the top foil, and this trend is more obvious at higher rotational speeds.

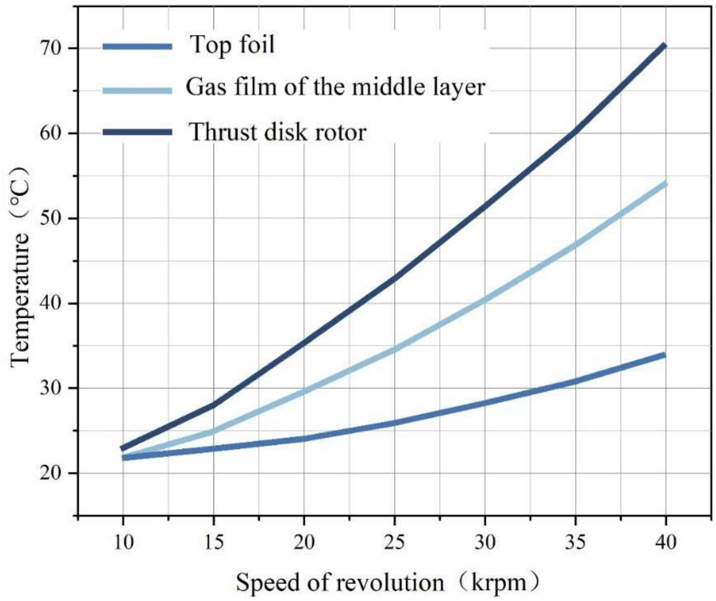

Fig. 9. The effect of the speed on the temperature of the thrust bearing

The effects of different initial minimum film thicknesses on the average temperatures of the top foil, the intermediate gas film and the thrust disk rotor of the foil gas thrust bearing are shown specifically in Fig. 10. In the calculation, the effect of cooling flow is not taken into account, and the rotor speed is 30 krpm. It can be seen from the figure that, with the decrease of the initial minimum film thickness (the axial bearing capacity increases), the temperatures of the top foil, the intermediate gas film and the rotor of the thrust disk basically increase linearly, and the magnitude of the increase is small. The temperature of each element of the foil gas thrust bearing increases linearly and slowly with the increase of axial load.

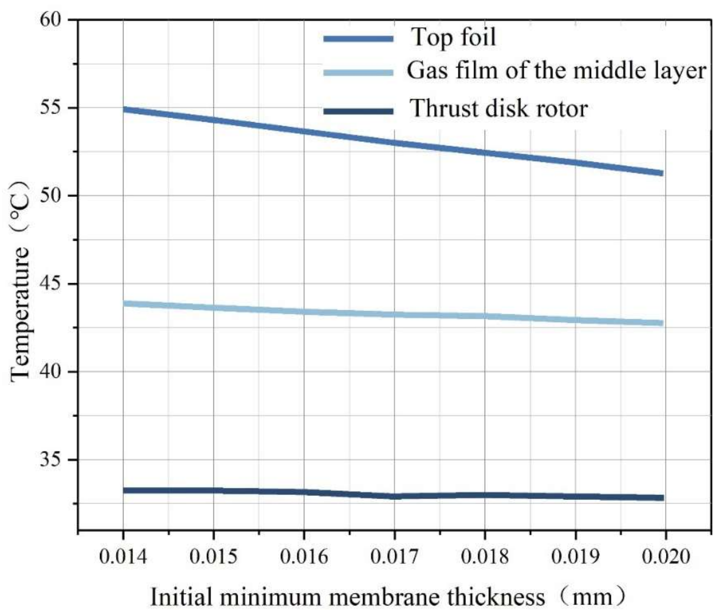

Fig. 10. The initial minimum film thickness effect

The one-dimensional temperature distribution along the radial direction of the thrust disk at different rotational speeds is shown in Fig. 11. From the figure, it can be seen that at the same rotational speed, the temperature of the thrust disk increases parabolically from the inner diameter to the outer diameter. With the increase of rotational speed, the temperature of the rotor of the thrust disk increases very obviously.

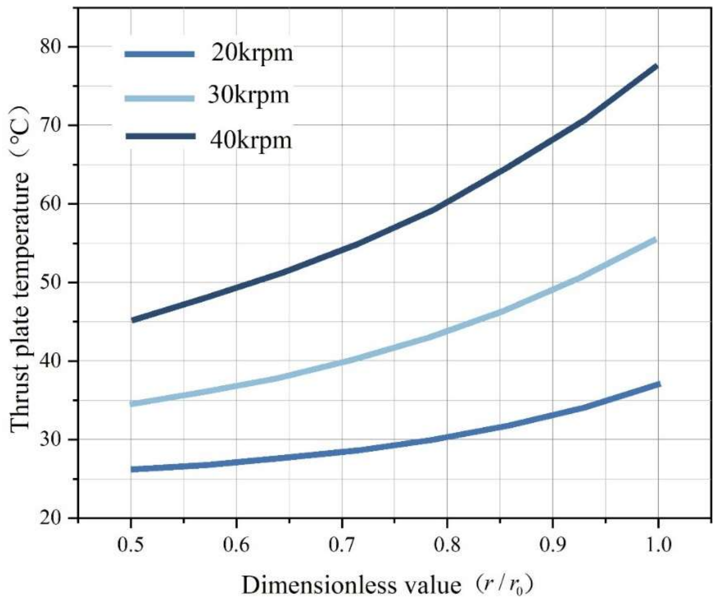

Fig. 11. Radial temperature distribution of thrust disc at different speed

The heat generated by the viscous friction of the lubricant film in foil gas thrust bearings may cause thermal deformation of the bearing, which has a very significant effect on its performance. Excessive temperatures in the lubricant film may even lead to thermal failure of the bearing. In engineering, temperature management measures are often used to reduce the internal temperature of the bearing by means of a cooling stream to the bottom of the top foil. The effect of cooling flow on the temperature of the foil gas thrust bearing at different speeds is shown in Figure 12. As shown in Fig. 12, the temperature with the cooling flow has a very obvious decrease compared with the average temperature of the top foil without cooling flow, and the average temperature of the top foil decreases rapidly with the increase of the cooling flow. The results show that the cooling flow to the bottom of the top foil is very effective in reducing the internal temperature of the bearing at different speeds.

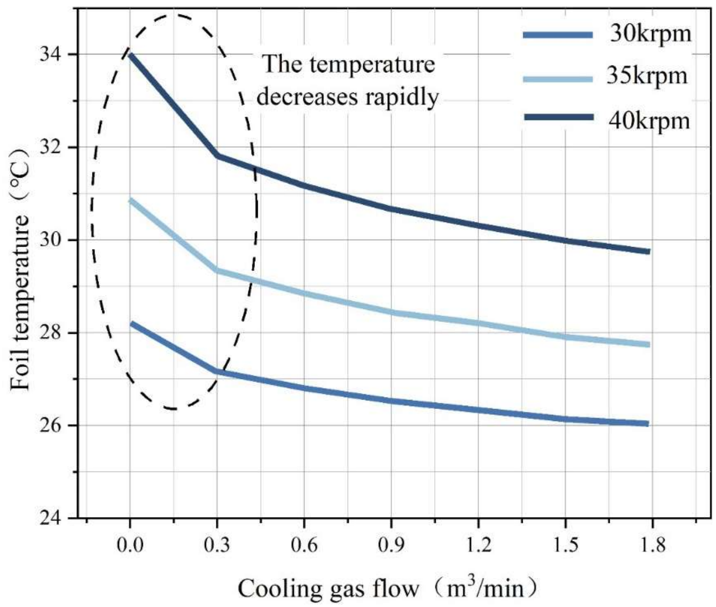

Fig. 12. The effect of cooling fluid flow on the foil temperature

5. Conclusion

This paper relies on the principle of thermodynamics, using the finite difference method to carry out an in-depth discussion and analysis of the thermodynamic behavior of high-speed devices. The research object of the core analysis of this paper is a typical representative of high-speed mechanical devices - gas bearings in high-speed rotating bearings. In the analysis of the impact of bearing performance, when the stiffness increases, the pressure change in the middle and rear of the bearing gradually flattens out, the temperature will also gradually increase, and the relative bearing capacity of the bearing is also consistent with the lack of changes in the average pressure, which is constantly decreasing. Obviously, the bearing design needs to consider the stiffness of the elastic foil, in order to ensure that the support structure under the premise of the original reduction of stiffness, to reduce the risk of high enough temperature when the bearing high-speed operation. As the number of bearings increases, the average pressure increases and the temperature of the air film rises, which has an impact on the performance of the bearings. Under the premise of ensuring high-speed operation, the bearing design should appropriately increase the number of bearings to improve the bearing capacity and reduce the risk of high temperature. Further in-depth analysis of the thermal characteristics of the bearing parameters, it can be understood that the rotational speed has a greater impact on the temperature of the air film, under the same load, the temperature of the air film increases rapidly with the increase in rotational speed. At the same rotational speed, the air film temperature increases linearly with the increase of load, but the effect of load on the air film temperature is much smaller than the effect of rotational speed on the air film temperature. The temperature of the lubricating air film can be effectively reduced by passing cooling gas at the bottom of the top foil.

References

[1] Özişik, M. N., Orlande, H. R., Colaço, M. J., & Cotta, R. M. (2017). Finite difference methods in heat transfer. CRC press.

[2] Shashkov, M. (2018). Conservative finite-difference methods on general grids. CRC press.

[3] Stynes, M., O'Riordan, E., & Gracia, J. L. (2017). Error analysis of a finite difference method on graded meshes for a time-fractional diffusion equation. SIAM Journal on Numerical Analysis, 55(2), 1057-1079.

[4] Lyu, P., Liang, Y., & Wang, Z. (2020). A fast linearized finite difference method for the nonlinear multi-term time-fractional wave equation. Applied Numerical Mathematics, 151, 448-471.

[5] Patidar, K. C. (2016). Nonstandard finite difference methods: recent trends and further developments. Journal of Difference Equations and Applications, 22(6), 817-849.

[6] Li, Z., Qiao, Z., & Tang, T. (2017). Numerical solution of differential equations: introduction to finite difference and finite element methods. Cambridge University Press.

[7] Lewis, G. N., Randall, M., Pitzer, K. S., & Brewer, L. (2020). Thermodynamics. Courier Dover Publications.

[8] Gaskell, D. R., & Laughlin, D. E. (2017). Introduction to the Thermodynamics of Materials. CRC press.

[9] Bejan, A. (2017). Evolution in thermodynamics. Applied Physics Reviews, 4(1).

[10] Turns, S. R., & Pauley, L. L. (2020). Thermodynamics: concepts and applications. Cambridge University Press.

[11] Meir, A., Offner, A., & Ramon, G. Z. (2018). Low-temperature energy conversion using a phase-change acoustic heat engine. Applied Energy, 231, 372-379.

[12] Lallart, M., Yan, L., Miki, H., Sebald, G., Diguet, G., Ohtsuka, M., & Kohl, M. (2021). Heusler alloy-based heat engine using pyroelectric conversion for small-scale thermal energy harvesting. Applied Energy, 288, 116617.

[13] Kleidon, A. (2024). The Second Law of Thermodynamics, Life and Earth‘s Planetary Machinery Revisited. Physics of Life Reviews.

[14] Rajnath, Y. K., Tiwari, S., & Kumar, V. (2024). Thermodynamics for Mechatronics. Computational Intelligent Techniques in Mechatronics, 41-81.

[15] Khalaj, A. H., & Halgamuge, S. K. (2017). A Review on efficient thermal management of air-and liquid-cooled data centers: From chip to the cooling system. Applied energy, 205, 1165-1188.

[16] Haghighat, A. K., Roumi, S., Madani, N., Bahmanpour, D., & Olsen, M. G. (2018). An intelligent cooling system and control model for improved engine thermal management. Applied Thermal Engineering, 128, 253-263.

[17] Liu, Z. K. (2020). Computational thermodynamics and its applications. Acta Materialia, 200, 745-792.

[18] Pokrovskii, V. N. (2020). Thermodynamics of Complex Systems: Principles and Applications. IOP Publishing.

[19] Swendsen, R. H. (2018). Thermodynamics of finite systems: a key issues review. Reports on Progress in Physics, 81(7), 072001.

[20] Barbour, A. (2021). The Rise of Thermodynamics: Mechanical Engineering and Byron's Poetic Machinery. ELH, 88(1), 107-131.

[21] Baker, J. E. (2022). Thermodynamics and Kinetics of a Binary Mechanical system: Mechanisms of muscle contraction. Langmuir, 38(51), 15905-15916.

[22] Benson, R. S. (2013). Advanced engineering thermodynamics: thermodynamics and fluid mechanics series. Elsevier.

[23] Ghosh, A., Niedenzu, W., Mukherjee, V., & Kurizki, G. (2018). Thermodynamic principles and implementations of quantum machines. Thermodynamics in the Quantum Regime: Fundamental Aspects and New Directions, 37-66.

[24] Osara, J. A. (2019). Thermodynamics of manufacturing processes—The workpiece and the machinery. Inventions, 4(2), 28.

[25] Jilong Yin,Huaqing Zhang,Mengmeng Liu,Xiaotao Yang,Pengrui Zhu & Yamin Wang. (2024). Numerical Simulation Analysis of Dock Bank Slopes' Soil–Water Interface Recognition and Monitoring Device Models Based on Heat Transfer Principles. Applied Sciences(18),8444-8444.

[26] Yu. K. Tovbin. (2024). The Second Law of Thermodynamics and the Surface Characteristics of Dispersed Systems. Russian Journal of Physical Chemistry A(12),2823-2827.

[27] Ramos A. J. A.,Almeida Júnior D. S. & Freitas M. M. (2022) .About polynomial stability for the porous-elastic system with Fourier's law.Zeitschrift für angewandte Mathematik und Physik(2).

[28] Md. Shorif Hossan,Trishna Datta & Md. Shafiqul Islam. (2024). Combining approach of collocation and finite difference methods for fractional parabolic PDEs. Partial Differential Equations in Applied Mathematics100921-100921.

[29] Christiaan Mommeyer,Geert Lombaert,Mattias Schevenels & Ole Sigmund. (2024). Taylor series approximations for faster robust topology optimization. Structural and Multidisciplinary Optimization(10), 181-181.